AIP | Applied Physics Letters

Imaging nanowire plasmon modes with two-photon polymerization

Christian Gruber, Andreas Hirzer, Volker Schmidt, Andreas Trügler, Ulrich Hohenester, Harald Ditlbacher, Andreas Hohenau, and Joachim R. Krenn

Citation: Applied Physics Letters **106**, 081101 (2015); doi: 10.1063/1.4913470
View online: http://dx.doi.org/10.1063/1.4913470
View Table of Contents: http://scitation.aip.org/content/aip/journal/apl/106/8?ver=pdfcov
Published by the AIP Publishing

Imaging nanowire plasmon modes with two-photon polymerization

Christian Gruber,[1] Andreas Hirzer,[2] Volker Schmidt,[2] Andreas Trügler,[1] Ulrich Hohenester,[1] Harald Ditlbacher,[1] Andreas Hohenau,[1] and Joachim R. Krenn[1,a)]
[1]*Institute of Physics, Karl-Franzens-University, Universitätsplatz 5, 8010 Graz, Austria*
[2]*Joanneum Research Materials—Institute for Surface Technologies and Photonics, Franz-Pichler Strasse 30, 8160 Weiz, Austria*

(Received 22 December 2014; accepted 12 February 2015; published online 23 February 2015)

Metal nanowires sustain propagating surface plasmons that are strongly confined to the wire surface. Plasmon reflection at the wire end faces and interference lead to standing plasmon modes. We demonstrate that these modes can be imaged via two-photon (plasmon) polymerization of a thin film resist covering the wires and subsequent electron microscopy. Thereby, the plasmon wavelength and the phase shift of the nanowire mode picked up upon reflection can be directly retrieved. In general terms, polymerization imaging is a promising tool for the imaging of propagating plasmon modes from the nano- to micro-scale. © *2015 AIP Publishing LLC*.
[http://dx.doi.org/10.1063/1.4913470]

Noble metal nanowires support plasmonic modes with propagation constants that scale inversely with the wire radius.[1] Plasmonic wires constitute thus optical waveguides without cut-off that could be miniaturized to nanoscale cross sections. Metallic damping limits, however achievable propagation lengths, which have been measured in the μm-range (for visible and near-infrared wavelengths) for silver and gold wires with diameters around 100 nm.[2,3] End face reflection turns a nanowire of length L into a Fabry-Perot resonator (for small L values to be considered as an optical antenna), with standing plasmon waves given by the resonance condition $k_{pl}L + \phi = m\pi$, with k_{pl} being the plasmon wave number, ϕ being the phase change of the plasmon wave upon reflection, and m being an integer. Such nanowire Fabry-Perot modes have been directly imaged with near field microscopy,[2,4] transmission electron microscopes equipped with electron energy loss spectroscopy (EELS)[5] and cathodoluminescence.[6] Analyzing measured mode patterns allowed, on one hand, to retrieve the plasmon wavelength $\lambda_{pl} = 2\pi/k_{pl}$ from the standing wave periodicity. Depending on the wire diameter, λ_{pl} was found to be significantly shorter than the related free space wavelength, in agreement with modelling.[2,4,5,7,8] The mode pattern allows to retrieve as well the reflection phase change as $\phi = 2(\pi - k_{pl}l)$, with "l" being the distance of the first standing wave antinode from the wire end face. The actual value of the reflection phase (alternatively expressed as an effective wire length with $\Delta L = \phi/k_{pl}$ or antenna reactance) addresses the important point of the resonance lengths of plasmonic nanowires and thus of their design.[9] ϕ depends rather strongly on the wire diameter and on λ_{pl}, as evident from the analytical solutions for cylindric gold[10] and silver[11] nanowires with flat end faces in a homogeneous medium. However, the details of the end face geometry are expected to play an important role for the reflection properties.[3,12,13] For experimental access, it is thus important to have a reliable experimental method with high spatial resolution at hand that is sensitive to the full plasmon field. Certainly, near field microscopy and EELS are very successful in this respect, but their sensitivity to specific plasmon field components and the potentially invasive character of a near field probe could hinder detailed analysis. In this letter, we report that two-photon (plasmon) polymerization (TPP) and subsequent electron microscopy imaging can be employed for imaging the plasmonic field along μm-long silver nanowires with high fidelity and relative ease. We furthermore show that λ_{pl} and ϕ can be directly retrieved from the plasmon-induced polymerization patterns.

Surface plasmon near fields can modify an embedding medium as a function of local plasmon intensity, as shown for the linear regime in an early work of Keilmann *et al.*[14] As a nonlinear process, TPP is capable of higher spatial resolution and it enables 3D lithography, as initially demonstrated for the direct writing of micro- and nanostructures with ultrafast laser sources.[15] More recently, the principle of TPP was applied to probe the near fields of localized plasmon fields around metal nanoparticles. First, nanoparticles deposited on a surface are covered by a resist film. Then, after exposure to laser pulses in the red or near-infrared spectral range the resist is developed and the (optionally metal coated) sample is imaged by scanning electron microscopy (SEM).[16–19] To apply this approach to the imaging of the propagating plasmon modes in nanowires, we use a commercial two photon direct-write system (Nanoscribe, Eggenstein-Leopoldshafen, Germany). 150 fs pulses from a fiber laser are emitted at a repetition rate of 100 MHz at a center wavelength of 780 nm, resulting in a spectral bandwidth of about 6 nm. The pulses are focused onto one end of the nanowires through a microscope objective (100×, numerical aperture 1.4) under polarization control. Light scattering from the other wire end is used as a guide for precise focusing as it evidences successful plasmon excitation and propagation along the wire.[2] The position of the sample relative to the laser focus is controlled with a piezoelectric stage. For exposure, we use the negative-tone resist IP-L (Nanoscribe) with a refractive index of 1.48 (at a wavelength of 780 nm). The nanowires on the glass substrate (refractive index 1.51 at a wavelength of 780 nm) are

a)Electronic mail: joachim.krenn@uni-graz.at

covered by the resist and thus embedded in an almost homogeneous environment. With an average laser power of 2–4 mW, we use exposure times per spot addressed by the laser focus of around 0.1 s. The exposed samples are developed in isopropanol for 5 min, leaving structures on the surface wherever the polymerization threshold was exceeded. Finally, the samples are coated with 5 nm chromium by thermal evaporation and imaged by SEM. The nanowires are fabricated on glass substrates by standard electron beam lithography. Electron exposure defines the wire geometries in a 60 nm thick poly(methyl metaacrylate) film that is covered by a few nm of aluminum for electric conductivity. After chemical development, the deposition of 50 nm of silver by thermal evaporation and lift-off, the wires with a cross section of $100 \times 50\,\text{nm}^2$ (± 2 nm) and lengths of 2, 3, and 4 μm remain on the glass substrate.

Fig. 1 shows overview SEM images of an exposed 3 μm long nanowire. The large polymerization volume around the focus position (left wire end) is due to the direct exposure to the laser pulses. The laser beam was polarized either parallel or perpendicular to the wire axis. Light scattering from the right wire end heralding plasmon propagation was only observed for parallel polarization, in agreement with expectations for the chosen wire geometry.[12] Indeed, for this polarization direction, we observe a regular polymer structure around the nanowire (Fig. 1(a)) that is absent in the case of pependicular polarization (Fig. 1(b)). Higher magnification SEM images from the right hand side of exposed nanowires (lengths 2, 3, and 4 μm) are depicted in Fig. 2, for the polarization direction parallel to the wire axis. The regular pattern around the wires is evident and we can readily assign it to a standing nanowire mode.[2] The polymerized volume is strongly confined to the wire surface, extending over only about 20 nm perpendicular to the metal surface. This value is much smaller that the voxel size achievable by TPP in a homogeneous medium and reflects the evanescent character of the plasmon field, in agreement with work on dielectric surfaces under total internal reflection illumination.[20] In addition, surface effects that lower the polymerization threshold close to a surface[21] might play a role.

By fitting a $\cos 2k_{pl}x$ function (x being the coordinate along the wire axis) to the standing wave patterns around 12 different nanowires of 2, 3, and 4 μm lengths, we retrieve an averaged value for the plasmon wavelength $\lambda_{pl} = 381 \pm 5$ nm

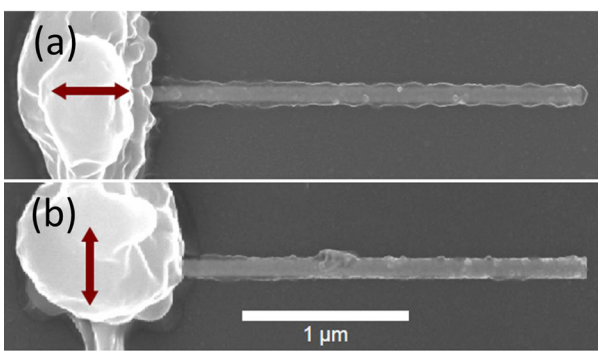

FIG. 1. SEM images of a 3 μm long silver nanowire, exposed to (a) parallely and (b) perpendicularly polarized laser pulses (as indicated by the double sided arrows) focused onto the left wire ends.

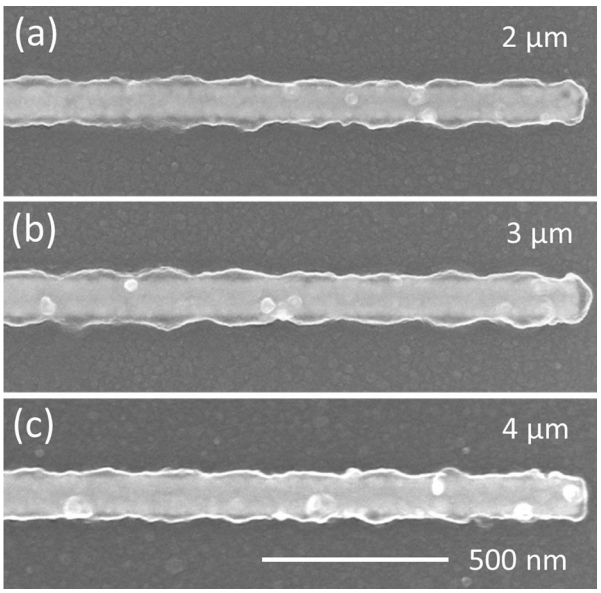

FIG. 2. SEM images of silver nanowires (a) 2, (b) 3, and (c) 4 μm long, exposed to parallely polarized laser pulses.

(see Fig. 3(a)). This value reflects the specific dispersion relation of nanowire plasmons and is in excellent agreement with values measured with other techniques on similar nanowires.[2,4,5,7,8] To corroborate our experimental result, we simulate the nanowire plasmon mode for the actual experimental parameters with the Matlab toolbox MNPBEM[22] that is based on the boundary element method.[23] The simulated result for a 2 μm long nanowire is plotted as an electric field strength map in Fig. 3(b) and as a charge map in Fig. 3(c). The simulated value of λ_{pl} of 390 nm is in very good agreement with the experimental finding.

Turning now to the reflection phase, we retrieve ϕ from the polymerized patterns, taking advantage of the different

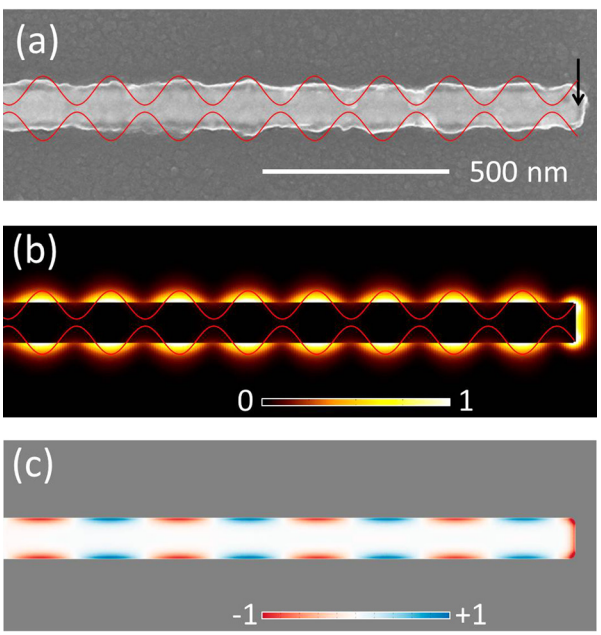

FIG. 3. Standing plasmon mode of a 2 μm long nanowire. (a) SEM image from Fig. 2(a), the arrow marks the nanowire end. (b) and (c) depict (normalized) simulated electric field strength and charge maps, respectively. The red lines are $\cos 2k_{pl}x$ fits to the standing wave pattern.

SEM contrasts of silver and polymer that makes the nanowire end clearly visible (arrow in Fig. 3(a)). We deduce a value of $\phi = 71 \pm 6°$, again as the averaged value from 12 nanowires. From the simulation in Fig. 3, we find $\phi = 71°$, corresponding very well to the experimental value. It is interesting to note that the reflection phase has been somewhat controversely discussed in the literature. In particular, different periodicities of the standing plasmon wave were found when comparing the outer and inner regions of nanowires.[4,5,24] These observations were at least partly assigned to the role of ϕ. As we do not recover this feature from our measurements, two explanations might apply. First, these studies investigated chemically synthesized nanowires that are deposited on the substrate from a solution. Such wires often show a slight bending that could cause the loosing of contact of some parts of the wire with the substrate. This might locally alter the plasmon mode profile and thus the standing wave pattern. By using lithographed nanowires we are not concerned by this point. Second, all mentioned studies were done with near field microscopy or EELS. Both techniques are sensitive to near field components rather that the overall field as in the case of TPP, and this specific sensitivity might give rise to deviations from strict periodicity, in particular, where experimental structures deviate from idealized geometries.

We note that standing plasmon patterns with similar polymerization contrast occur for all three nanowire lengths (2, 3, and 4 μm). Indeed, for these lengths the retrieved values of λ_{pl} and ϕ fulfill the resonance condition for nanowire modes as defined above quite well. Due to the rather high damping of the nanowire plasmon modes,[25] it is, however, not critical to meet this condition precisely.

For further quantitative analysis, a possible refractive index change of the resist during exposure has to be considered. From the available data for negative-tone resists (e.g., Refs. 20 and 26), we estimate the effects of cross-linking and shrinkage on the refractive index to 1%–3%. The impact of this effect on the measured plasmon wavelength depends on the dynamics of the index change, which requires further investigation.

In summary, we have shown that the plasmon modes of μm-long nanowires can be imaged and characterized with TPP and SEM imaging. From the imaged TPP pattern, λ_{pl} and ϕ can be retrieved. Imaging over μm length with a lateral size of the polymerized volumes <20 nm illustrates the power of this method that thus seems applicable to image any type of nano-optical fields with high spatial resolution and high throughput. However, quantifying the plasmon fields in terms of field enhancement and profile is not straightforward and requires dedicated further measurements.[18,19]

Financial support is acknowledged from the FWF SFB NextLite (F4905-N23 and F4906-N23).

[1]J. Takahara, S. Yamagishi, H. Taki, A. Morimoto, and T. Kobayashi, Opt. Lett. **22**, 475 (1997).
[2]H. Ditlbacher, A. Hohenau, D. Wagner, U. Kreibig, M. Rogers, F. Hofer, F. R. Aussenegg, and J. R. Krenn, Phys. Phys. Lett. **95**, 257403 (2005).
[3]P. Kusar, C. Gruber, A. Hohenau, and J. R. Krenn, Nano Lett. **12**, 661 (2012).
[4]J. Dorfmueller, R. Vogelgesang, R. T. Weitz, C. Rockstuhl, C. Etrich, T. Pertsch, F. Lederer, and K. Kern, Nano Lett. **9**, 2372 (2009).
[5]D. Rossouw, M. Couillard, J. Vickery, E. Kumacheva, and G. A. Botton, Nano Lett. **11**, 1499 (2011).
[6]E. J. R. Vesseur, R. de Waele, M. Kuttge, and A. Polman, Nano Lett. **7**, 2843 (2007).
[7]J. Dorfmueller, R. Vogelgesang, W. Khunsin, C. Rockstuhl, C. Etrich, and K. Kern, Nano Lett. **10**, 3596 (2010).
[8]V. D. Miljkovic, T. Shegai, P. Johansson, and M. Kall, Opt. Express **20**, 10816 (2012).
[9]L. Novotny, Phys. Rev. Lett. **98**, 266802 (2007).
[10]R. Gordon, Opt. Express **17**, 18621 (2009).
[11]R. Kolesov, B. Grotz, G. Balasubramanian, R. J. Stöhr, A. A. L. Nicolet, P. R. Hemmer, F. Jelezko, and J. Wachtrup, Nat. Phys. **5**, 470 (2009).
[12]Z. Li, K. Bao, Y. Fang, Y. Huang, P. Nordlander, and H. Xu, Nano Lett. **10**, 1831 (2010).
[13]S. Bin Hasan, R. Filter, A. Ahmed, R. Vogelgesang, R. Gordon, C. Rockstuhl, and F. Lederer, Phys. Rev. B **84**, 195405 (2011).
[14]F. Keilmann, K. W. Kussmaul, and Z. Szentirmay, Appl. Phys. B **47**, 169 (1988).
[15]S. Kawata, H. Sun, T. Tanaka, and K. Takada, Nature **412**, 697 (2001).
[16]A. Sundaramurthy, P. Schuck, N. Conley, D. Fromm, G. Kino, and W. Moerner, Nano Lett. **6**, 355 (2006).
[17]N. Murazawa, K. Ueno, V. Mizeikis, S. Juodkazis, and H. Misawa, J. Phys. Chem. C **113**, 1147 (2009).
[18]C. Deeb, X. Zhou, R. Miller, S. K. Gray, S. Marguet, J. Plain, G. P. Wiederrecht, and R. Bachelot, J. Phys. Chem. C **116**, 24734 (2012).
[19]T. Geldhauser, A. Kolloch, N. Murazawa, K. Ueno, J. Boneberg, P. Leiderer, E. Scheer, and H. Misawa, Langmuir **28**, 9041 (2012).
[20]C. Ecoffet, A. Espanet, and D. Lougnot, Adv. Mater. **10**, 411 (1998).
[21]D. Kunik, S. J. Luduena, S. Costantino, and O. E. Martinez, J. Microsc. **229**, 540 (2008).
[22]U. Hohenester and A. Trügler, Comp. Phys. Commun. **183**, 370 (2012).
[23]F. de Abajo and A. Howie, Phys. Revs. B **65**, 115418 (2002).
[24]O. Nicoletti, M. Wubs, N. A. Mortensen, W. Sigle, P. A. van Aken, and P. A. Midgley, Opt. Express **19**, 15371 (2011).
[25]A. Hohenau, P. Kusar, C. Gruber, and J. R. Krenn, Opt. Lett. **37**, 746 (2012).
[26]B. Ong, X. Yuan, S. Tao, and S. Tjin, Opt. Lett. **31**, 1367 (2006).